



ELSEVIER

Contents lists available at ScienceDirect

Comptes Rendus Chimie

www.sciencedirect.com



Full paper/Mémoire

Stability and dynamics of silicate/organic hybrid micelles

Stabilité et dynamique de micelles hybrides silicates/organiques

Andrew Kacheff, Eric Prouzet*

University of Waterloo, Chemistry Department, 200 University Avenue W, Ontario, N2L 3G1, Canada

ARTICLE INFO

Article history:

Received 14 July 2016

Accepted 3 November 2016

Available online xxx

Keywords:

Micelles

Hybrid micelles

DLS

Fluorescence

Mesophase

Silica

Mesoporous

ABSTRACT

The formation of silicate/organic hybrid micelles is an important milestone in the two-step synthesis of mesoporous silica with polyethyleneoxide (PEO) nonionic structure directing agents (C.R. Chimie 8 (2005) 579). Unlike many inorganic/organic hybrid micelles, these objects have the inorganic component as a diffuse layer positioned at the periphery of the initial micelles and interacting with the hydrophilic polyoxyethylene palisade. We studied how this additional inorganic layer can modify the structure and dynamics of micelles prepared with different types of nonionic surfactants using steady-state and time-resolved fluorescence and dynamic light scattering. Our results show that these hybrid micelles still possess a versatile behavior, which allows them to adapt reversibly to temperature changes. This silicate layer tends to stabilize and consolidate the micelle structure, especially close to the cloud point of critical micelle temperature for polypropyleneoxide (PPO)-based triblock copolymers. Their internal structure is only slightly disturbed by the silicate layer, which reduces the molecular exchanges a little bit. Among other results, we managed to elucidate why mesoporous silica prepared with Pluronic P123, according to our synthesis, stands a dramatic structural change from wormhole to hexagonal structure at 40 °C. Our dynamic light scattering study shows that 40 °C is a critical temperature corresponding to a sphere-to-rodlike structural transition of hybrid micelles, which is not observed with pure micelles.

© 2016 Académie des sciences. Published by Elsevier Masson SAS. All rights reserved.

RESUME

La formation de micelles hybrides organiques/inorganiques est une étape importante dans la synthèse en deux étapes des silices mésoporeuses obtenues avec des agents structurants de type copolymère diblock polyéthylène glycol (PEG) (C. R. Chimie 8 (2005) 579). Contrairement à la plupart des objets décrits comme micelles hybrides organique/inorganique, ces objets micellaires présentent leur composant inorganique positionné comme une couche diffuse à la périphérie de la micelle initiale, et en interaction avec la couronne hydrophile formée des chaînes PEG. Nous avons étudié par fluorescence en mode statique et résolu en temps, ainsi que par spectroscopie de photocorrélation, comment l'ajout d'une telle couche inorganique peut modifier la structure et la dynamique de micelles préparées avec différents types de tensioactifs non ioniques. Nos résultats démontrent que ces micelles hybrides possèdent un comportement très versatile, leur permettant de s'adapter réversiblement aux variations de température. Ces couches de silicate tendent à stabiliser et renforcer la structure micellaire, en particulier lorsqu'on s'approche du point de trouble (CP) et de la température micellaire critique (CMT) pour les copolymères triblock à base de polypropylène

Mots-clés:

Micelles

Micelles hybrides

DLS

Fluorescence

Mésophase

Silice

Mésoporeux

* Corresponding author.

oxyde. Leur structure interne est déstabilisée légèrement par la couche de silicate, avec pour conséquence une faible réduction des échanges moléculaires. Entre autres résultats, nous sommes parvenus à trouver la raison pour laquelle les silices mésoporeuses préparées avec du Pluronic™ P123, selon notre mode de synthèse, sont affectées par un changement structural majeur à 40 °C, avec la formation d'une structure hexagonale en nid d'abeille. Notre étude par spectroscopie de photocorrélation montre que 40 °C correspond à une température critique avec une transition de micelle sphérique en micelle allongée, une telle transition n'étant pas observée pour les solutions micellaires pures.

© 2016 Académie des sciences. Published by Elsevier Masson SAS. All rights reserved.

1. Introduction

There is an increasing demand of integration of functionalities in nanomanufacturing of advanced materials. This leads to a growing trend in creating nanobuilding blocks with integrated components at the molecular scale. In this domain, which belongs to integrative chemistry or syntheses [1–3], the need of intimate interactions between building blocks becomes more and more expected.

Among the list of potential nanobuilding blocks, hybrid micelles offer this type of intimate combination of composite nanostructures and specific interactions at the mesoscale. Organic hybrid micelles combine amphiphiles and polymers [4,5], whereas inorganic/organic hybrid micelles are usually made of nanoparticles embedded in the core of the micelle and wrapped with amphiphiles [6–10]. We have reported how mesoporous silica can be synthesized with a fine-tuning of pore size, when nonionic amphiphilic copolymers are used in combination of a fine adjustment of the synthesis temperature [11]. This fine-tuning of the silica mesostructure is allowed by the intermediary formation of stable silicate/surfactant hybrid micelles [12]. Unlike most of the hybrid organic/inorganic micelles reported so far, these hybrid micelles have their inorganic component as a diffuse shell of weakly reticulated silicate oligomers around the organic core. This diffuse layer of silicates should confer a higher dynamics to the hybrid micelles than when nanoparticles are involved. Unlike ionic surfactants, polyethyleneoxide (PEO)-based diblock copolymer micelles possess specific properties, because of the nature of the hydrophilic interactions, with by example, the cloud point (CP) temperature corresponding to the temperature beyond which the hydrophilic behavior is lost as a result of the breakage of H-bonds. As the temperature rises, the PEO chains progressively dehydrate, resulting in chain stretching, and leading to a reversible micelle size increasing. Another property of PEO-polypropyleneoxide (PPO)-based triblock copolymers is the critical micelle temperature (CMT), the minimum temperature below which the PPO chains are not hydrophobic enough.

These hybrid micelles are the fundamental intermediates of our two-step synthesis pathway, where small changes in synthesis parameters, especially temperature, can lead to drastic modifications of the final material [13]. Therefore, the full description of the structure of these hybrid micelles and their temperature-dependent dynamics is an important requirement for the complete understanding of the material

mesostructuring, and a way to explore how different nonionic templates can direct the formation of different mesoporous structures. In the present study, we used temperature-dependent dynamic light scattering (DLS) to follow the micelle size evolution. Steady-state and time-resolved fluorescence studies were used to probe the internal structure and dynamics of these hybrid micelles and explore how the presence of the outer silicate shell modifies these characteristics, compared with pure micelles.

2. Experimental section

2.1. Materials

Except when specified, all chemicals were purchased from Sigma Aldrich and used as received. The chemicals used for the preparation of the hybrid micelles combined a nonionic surfactant selected among several are as follows: Tergitol 15S12 (polyoxyethylene (12) pentadecyl ether $\text{CH}_3(\text{CH}_2)_{14}(\text{EO})_{12}$; $d = 0.993$; $M_w = 740$ g; CP = 89), Tergitol 15-S-30 (polyoxyethylene (30) pentadecyl ether $\text{CH}_3(\text{CH}_2)_{14}(\text{EO})_{30}$; $d = 1.055$; $M_w = 1520$ g; CP > 100 °C), Tergitol NP-10 (nonylphenol ethoxylate; $d = 1.060$, $M_w = 645$ g; CP ≈ 63 °C), Tween 20 (polyoxyethylene (20) sorbitan monolaurate; $d = 1.095$; $M_w = 1230$ g; CP = 76 °C), Brij 98 (polyoxyethylene (20) oleyl ether; $d = 1.070$; $M_w = 1150$ g; CP > 100 °C), Brij 35 (polyoxyethylene (24) dodecyl ether; $d = 1.060$; $M_w = 1198$ g; CP > 100 °C), Pluronic P123 (triblock copolymer $(\text{PEO})_{20}-(\text{PPO})_{70}-(\text{PEO})_{20}$; $d = 1.040$; $M_w = 5800$ g; CP = 90 °C), and tetraethylorthosilicate (TEOS: $\text{Si}(\text{CH}_2\text{CH}_3)_4$; $M_w = 208$ g). The pH of water (deionized water, PALL Cascada IX with 18 M Ω quality) was adjusted with hydrochloric acid (Fisher Scientific) at pH 2. Fluorescence studies used tetrahydrofuran (Caledon) and pyrene.

2.2. Sample preparation

Silica hybrid micelles were prepared by first dissolving the surfactant into a solution of hydrochloric acid diluted to pH 2 under magnetic stirring. After full dissolution of the surfactant, TEOS was added at room temperature to the solution dropwise under stirring at 500 rpm. The solution turned cloudy upon immediate addition of the TEOS. The solution remained under stirring until it turned clear within 10 min, as a result of TEOS hydrolysis [12]. The concentration of surfactant was kept constant at 20 mM.

For DLS studies, the concentration in TEOS was set to 200 mM (TEOS/surf. = 10) or 400 mM (TEOS/surf. = 20). Samples are referred in the following as **X/DLS/N** (**X** = surfactant name, **N** = TEOS/surf.).

Only Tergitol 15S12 was used for the steady-state fluorescence studies, with a concentration in TEOS set to 100 mM (TEOS/surf. = 5), 200 mM (TEOS/surf. = 10), or 300 mM (TEOS/surf. = 15). For steady-state fluorescence analysis, each of these initial solutions was diluted with water at pH 2 to produce series of samples at different concentrations with a given TEOS/surf. ratio. Samples (10 mL) were prepared with each sample diluted at the following concentrations in surfactant: 0.04, 0.047, 0.062, 0.10, 0.12, 0.14, 0.18, 0.21, 0.28, and 0.84 mM. As the amount of pyrene to be added is very small, pyrene was dissolved in tetrahydrofuran (THF) and diluted until an absorbance of approximately 0.2 was reached. This solution (0.5 g) was evaporated, and the diluted solutions of silica hybrid micelle were then poured into the vial containing the pyrene after evaporation of THF. The solutions were left under shaking for 3 h. Samples for the steady-state fluorescence studies are referred in the following as **T15S12/FSS/N/c** (**N** = TEOS/surf., **c** = surf. concentration in mM).

Samples for the time-resolved fluorescence studies are referred in the following as **T15S12/FLT/N/c** (**X** = surfactant name, **N** = TEOS/surf., **c** = concentration in mM). Samples for time-resolved fluorescence analysis were prepared with each initial TEOS/surf. ratio (**T15S12/FLT/N/0.52**, **N** = 0, 5, 10, 15), and diluted with water (pH 2) to a surfactant concentration of 0.52 mM. A 0.13 mM solution of pyrene in THF was prepared (absorbance 5.0). Increasing amounts (0.083, 0.166, 0.249, 0.332, 0.498, and 0.664 g) of this solution were evaporated, and the dried pyrene was mixed with the solutions of silica hybrid micelle by pouring these solutions into the vial containing the pyrene. These solutions were left under shaking for 3 h.

2.3. Methods

The size of surfactant micelles and silica hybrid micelles was measured by DLS with a Vasco DLS (Cordouan Technology). The diffusion coefficient of micelles was measured, and the hydrodynamic diameter was deduced using the Stokes–Einstein equation

$$D = \frac{k_B T}{3\pi\eta D_h} \quad (1)$$

where D is the diffusion coefficient, η the viscosity of the solution, T the temperature, k_B the Boltzmann constant, and D_h the hydrodynamic diameter. A 65 mW monomode red laser ($\lambda = 658$ nm) with variable intensity was used. Measurements were conducted at various temperatures (from 15 to 65 °C inclusive at 10 °C intervals) with the detector set at 135°. The experimental parameters (sampling time and number of channels) were adjusted for each sample to obtain the entire autocorrelation function. Final values reported result from a statistical analysis with 10 recordings performed at each temperature. In Figs. 1–5, the filled marks correspond to the average value resulting from the 10 individual recordings, and unfilled marks correspond to

values for each individual recording. The two models used to fit the autocorrelation function were a single size cumulant fit and a Padé–Laplace fit. The autocorrelation function for every single scan was fitted with the multisize Padé–Laplace fitting model [14] to check the existence of any polydispersity. Single size results were obtained for all samples. For every sample, the statistical size distribution was deduced from sizes obtained for every single scan, and the average value was deduced from this size distribution.

Steady-state fluorescence measurements were carried out to obtain the fluorescence spectra of the loaded silica hybrid micelles with a Photon Technology International (PTI) LS-100 steady-state fluorometer equipped with an Ushio UXL-75Xe xenon arc lamp and a Photon Technology International 814 photomultiplier detection system.

Steady-state fluorescence measurements were used to measure the I_E/I_M ratio of the fluorescence intensity of the excimer (I_E) over that of the monomer (I_M) to determine the critical micelle concentration (CMC). Fig. S1 (see Electronic Supplementary data) displays the normalized fluorescence spectra for the different surfactant concentrations. The I_M value was determined from the average intensity between 368 and 374 nm, and the I_E value was determined from the average intensity between 500 and 530 nm.

Fluorescence decays were acquired with an IBH time-resolved fluorometer fitted with a 340 nano-LED light source. The pyrene solutions were excited at 338 nm, and the fluorescence emission was monitored at 370 nm with a 365 nm cutoff filter to minimize stray light scattering from reaching the detector. Background and light scattering corrections were applied to fit the fluorescence decays with Eq. (2).

$$[\text{Py}^*]_{(t)} = [\text{Py}^*]_{(t=0)} \times \exp\left[-t/\tau_M - \langle n \rangle (1 - \exp(-k_q t))\right] \quad (2)$$

In Eq. (2), $[\text{Py}^*]_{(t)}$ is the time-dependent concentration of excited pyrenes, $[\text{Py}^*]_{(t=0)}$ is the initial concentration of excited pyrene, τ_{Py} is the natural lifetime of the excited pyrene, $\langle n \rangle$ is the average number of pyrenes per micelle, and k_q is the excimer formation rate constant for a micelle containing one excited pyrene and one ground-state pyrene. The fitting routine fitted the decays by optimizing the parameters τ_{Py} , $\langle n \rangle$, and k_q whose values have been reported in Table S1. A plot of $\langle n \rangle$ as a function of pyrene concentration yielded good straight lines whose slopes were calculated to determine the aggregation number of the micelles (N_{agg}) according to Eq. (3), where CMC is of the surfactant.

$$N_{\text{agg}} = \text{slope} \times ([\text{surfactant}] - \text{CMC}) \quad (3)$$

3. Results and discussion

3.1. Stability of hybrid micelles

The steady-state fluorescence analysis of pyrene dissolved into the silicate hybrid micelles confirms that neither the CMC nor the micelle structure is affected overall, upon addition of silicate.

We added pyrene to a series of **T15S12/FSS/N/c** ($N = \text{TEOS/surf.}: 0, 5, 10, 15, c = [\text{surf.}]: 0.04\text{--}0.84 \text{ mM}$) silica hybrid micelles to determine the influence of the silicate palisade on the CMC. This value was quantified by plotting the I_E/I_M ratio as a function of surfactant concentration (Fig. S1). This ratio is expected to increase with the surfactant concentration up to the CMC and decrease beyond it. Excimers are generated only when micelles are present in small numbers that can concentrate the few pyrene molecules in the solution. As the surfactant concentration reaches the CMC, the quantity of micelles able to host pyrene molecules increases and a maximum I_E/I_M ratio is reached around the CMC. As the surfactant concentration increases past the CMC, the I_E/I_M ratio begins to decrease because of the increasing dilution of available pyrene molecules within an increasing number of micelles, which hampers the formation of excimers. As a result, the surfactant concentration at the I_E/I_M peak maximum defines the CMC.

Fig. 1 is a plot of the I_E/I_M ratio as a function of the surfactant concentration, for different values of N (TEOS/surf.). The maximum I_E/I_M value is observed for the surfactant alone at $[\text{surf.}] = \text{CMC} = 0.11 \text{ mM}$. The I_E/I_M ratio passed through a maximum at the same surfactant concentration of 0.12 mM for the silicate hybrid micelles regardless of the amount of TEOS present. This similar value indicates that the presence of the silicate layer has little effect on the ability of pyrene to form excimer in the silica hybrid micelles and form excimers. It also suggests that the viscosity of the environment probed by pyrene is little affected by the amount of TEOS in the solution. The silicate outer shell forms a permeable layer, which does not affect the accessibility of the solvent to the micelles, and does not create any specific constraint onto the micelle itself.

We calculated also the I_1/I_3 ratio deduced from peak intensities at 370 and 382 nm, respectively (Fig. S2). A plot of the I_1/I_3 ratio as a function of surfactant concentration is displayed in Fig. 2 for different values of N . Changes in the I_1/I_3 ratio reflect changes in the polarity of the environment probed by pyrene (I_1/I_3 varies from 1.87 from water to 0.66 in cyclohexane) [15]. The I_1/I_3 ratio decreases as the concentration in surfactant increases up to a 0.11 mM

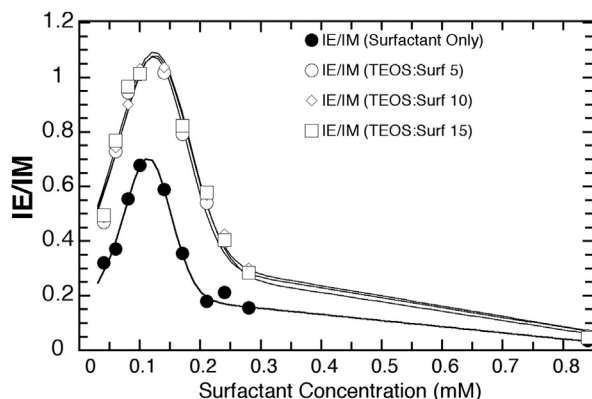


Fig. 1. I_E/I_M ratio at various TEOS/surfactant ratios.

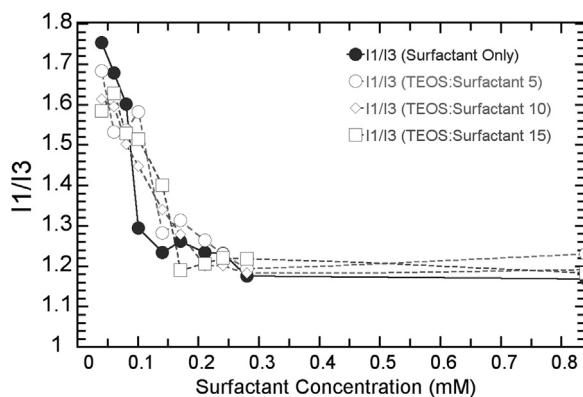


Fig. 2. I_1/I_3 ratios calculated for **T15S12/FSS/N/c** series for all concentrations.

concentration beyond which the I_1/I_3 ratio remains constant. The results demonstrate that more pyrene molecules, initially dissolved in water (the polar environment), enter the micelle (the nonpolar hydrophobic environment) as the surfactant concentration increases. For a concentration of 0.11 mM , all pyrene has entered the core of the micelles. Here again, we observe that the presence of the silicate layer ($N = 5, 10, 15$) does not modify the trend observed with pure micelles. This means that the presence of the silicate shell affects neither the diffusive incorporation of pyrene from water into the micellar core nor the local polarity of the micellar core probed by pyrene.

3.2. Structure and intermicellar interactions

We studied how the presence of the silicate outer shell can modify the aggregation number of surfactant molecules in the silica hybrid micelles compared with pure micelles. Within experimental error, the time-resolved fluorescence measurements demonstrate that the aggregation number of surfactant molecules is not affected by the presence of silicates. For T15-S-12/0/0.52 (see Table S1), an aggregation number of 69 ± 2 was obtained for the surfactant alone. With the addition of silicate, the aggregation number equaled $71 (\pm 2)$, $77 (\pm 2)$, and $74 (\pm 3)$ for N values of 5, 10, 15, respectively. The rate constant of excimer formation decreased slightly in the presence of TEOS taking values of $1.09 (\pm 0.04)$, $0.91 (\pm 0.05)$, $1.00 (\pm 0.04)$, and $0.89 (\pm 0.05) \times 10^7 \text{ s}^{-1}$ for N values of 0, 5, 10, and 15, respectively. Similarly, the natural lifetime of pyrene took a slightly larger value in the presence of TEOS, τ_M being equal to $186 (\pm 5)$, $205 (\pm 14)$, $197 (\pm 9)$, and $214 (\pm 11) \text{ ns}$ for N values of 0, 5, 10, and 15, respectively. These results are internally consistent. The slightly lower aggregation number, faster kinetics of pyrene excimer formation in the micelles, and shorter pyrene lifetime for the surfactant without TEOS compared with the hybrid micelles must be a result of the loose interactions that take place between the surfactant and TEOS. The hybrid micelles are slightly larger, thus reducing the rate constant of excimer formation, which is inversely proportional to the micellar volume and increase the pyrene lifetime by minimizing pyrene contacts with water.

3.3. Temperature-dependent dynamics of hybrid micelles

DLS results demonstrate that the presence of the silicate shell can affect in different ways the temperature-dependent evolution of the hybrid micelles, which mostly depends on the concentration in silicate, and the nature of copolymer. All samples are named according to the **X/DLS/N** nomenclature, with **X** being the surfactant name, and **N** the TEOS over surfactant molar ratio being equal either to 10 or 20. DLS measurements were done by progressively increasing the temperature in the measurement chamber from 15 to 65 °C and then cooling down. When possible, the statistical analysis (10 runs, final result averaged) was conducted.

Fig. 3a and b shows the size evolution for **T15S12/DLS/10** and **T15S12/DLS/20**, respectively, as a function of temperature. The hydrodynamic diameter of pure Tergitol 15S12, combining a PEO and a linear alkyl chain, varies linearly and reversibly from 8 to 18 nm as the temperature varies from 15 to 65 °C. Hybrid micelles prepared with a TEOS/surfactant ratio of 10 (**T15S12/DLS/10**) show a similar linear temperature dependent evolution, only shifted to larger sizes (10–20 nm) (Fig. 3a). As the silicate shell increases (**T15S12/DLS/20**) (Fig. 3b), a similar size evolution is still observed (11–14 nm) within a narrower size range, probably as a result of higher confinement. These results show that hybrid micelles made with an outer diffuse shell of silicates interacting with the hydrophilic PEO palisade present the same dynamic behavior than pure micelles, with a reversible temperature-induced adaptive size.

Similar analyses with long alkyl chain nonionic PEO surfactants (Brij 98: 20 EO; Brij 35: 24 EO; Tergitol 15S30: 30 EO) are reported in Fig. S3. Compared with Tergitol 15S12 (12 EO), the temperature-induced size evolution follows the same trend, with some fluctuations, when temperature increases. It is worth noticing that upon cooling, the same linear trend is observed for all surfactants. It seems from these results that the additional silicate shell consolidates the micelle structure, the first temperature ramp being used as an “annealing” mechanism.

We carried out the same type of analyses with hybrid micelles made with an aryl-alkyl-PEO surfactant (Tergitol NP-10) (Fig. 4a and b). This analysis reveals another important feature of silicate hybrid micelles, compared with pure surfactants. Tergitol NP-10 has a CP temperature in the 60–70 °C temperature range. We observe, as expected, that the hydrodynamic diameter of pure Tergitol NP-10 micelles increases drastically with temperature as the temperature comes closer to the CP (10–40 nm between 15 and 65 °C). The same temperature-induced size evolution as for hybrid micelles prepared with Tergitol 15S12 (Fig. 3) is also observed for the hybrid micelles prepared with Tergitol NP-10 (Fig. 4). However, the contribution of silicate oligomers on this temperature-dependent size evolution is dramatically enhanced at high temperature compared with the pure surfactant micelles (25 nm for hybrid micelles vs 40 nm for pure micelles). In this case, the silicate oligomers provide an additional contribution, which reinforces the micelle structure as it comes near the CP. These results show that the hybrid micelles made with Tergitol NP-10 still display the adaptive behavior to temperature, observed with others nonionic surfactants, but with a size evolution less sensitive to the dehydration of EO groups than for pure surfactants micelles. It is difficult for now to discriminate between the two possible hypotheses: (1) the silicate shell confines the internal hydrophilic palisade and controls the size evolution, and/or (2) the presence of silicates within the hydrophilic PEO shell keeps water molecules in their vicinity, which reduces the temperature-induced dehydration of PEO chains.

For another class of copolymers tested in this study (Tween 20) (Fig. 4c and d), we observe the same evolution with temperature. Unlike Tergitol 15S12, the temperature evolution of the micelle size is limited: 10–15 nm from 15 to 65 °C, and silicate hybrid micelles show the same limited evolution.

One of the most interesting results is obtained with the Pluronic P123 copolymer (Fig. 5). First, we observe that the size of hybrid micelles is smaller than the size of pure micelles. Pluronic P123 is a PEO–PPO–PEO triblock

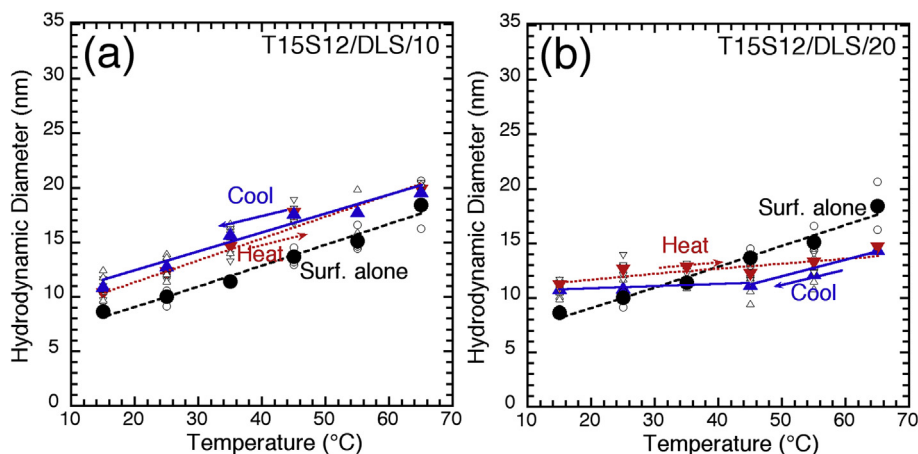


Fig. 3. Temperature evolution of the hydrodynamic diameter for pure Tergitol 15S12 micelles (filled circles), and hybrid micelles upon heating (down triangles) and cooling (up triangles) for (a) **T15S12/DLS/10** and (b) **T15S12/DLS/20** (lines are for visual help).

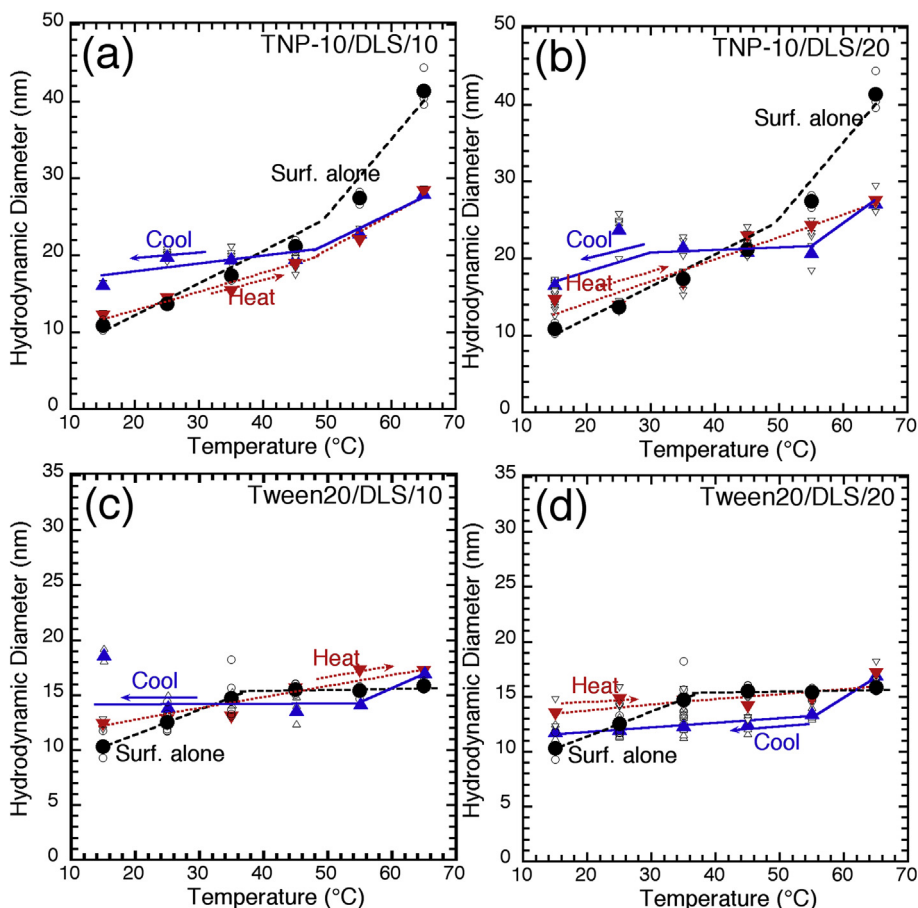


Fig. 4. Temperature evolution of the hydrodynamic diameter for an alkyl-aryl-PEO surfactant (Tergitol NP-10) and a sorbitan monolaurate (Tween 20) (pure micelles, filled circles; hybrid micelles upon heating, down triangles; hybrid micelles upon cooling, up triangles) and different TEOS/surf. molar ratios (10 and 20): (a) TNP-10/DLS/10, (b) TNP-10/DLS/20, (c) Tween 20/DLS/10, (d) Tween 20/DLS/20 (lines are for visual help).

copolymer, with a CMT in the 15 °C range. At low temperature, copolymers are still rather hydrophilic and ill-defined aggregates are expected, as observed here. When temperature increases (25 °C), PPO chains become more

hydrophobic, and the actual self-assembly mechanism can take place, giving well-defined mesoscopic objects. We can confirm this trend by just comparing the dispersion of individual measurements at 15 (broad distribution) and 25 °C

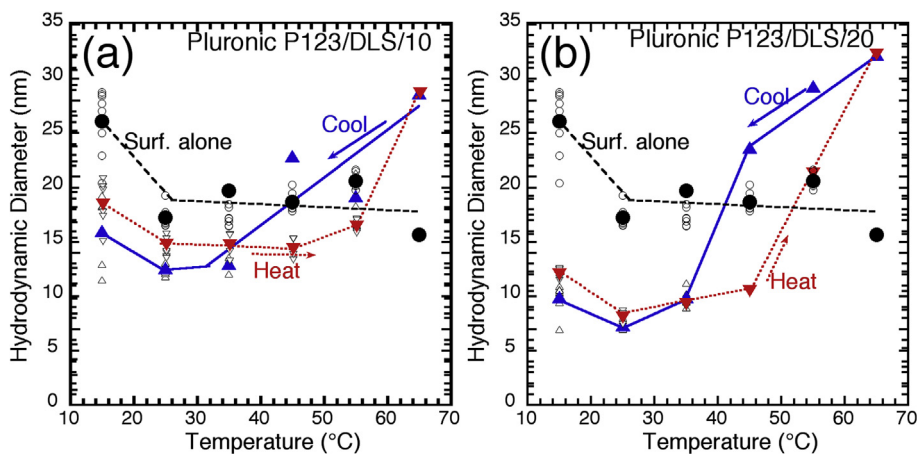


Fig. 5. Temperature evolution of the hydrodynamic diameter for pure Tergitol 15S12 micelles (filled circles), and hybrid micelles upon heating (down triangles) and cooling (up triangles) for (a) T15S12/DLS/10 and (b) T15S12/DLS/20 (lines are for visual help).

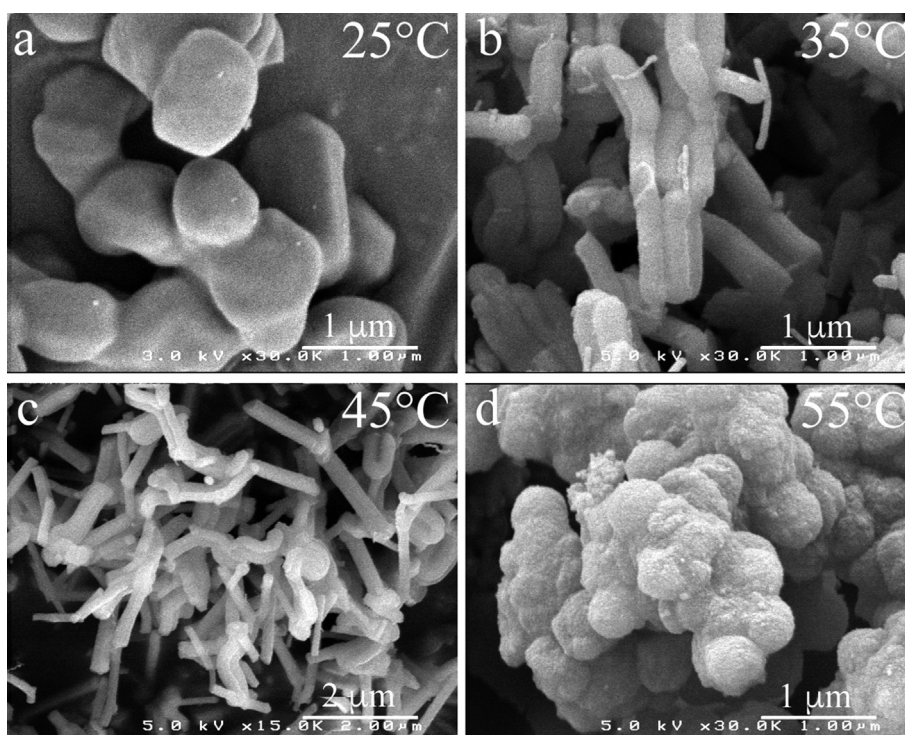


Fig. 6. SEM micrographs of mesoporous silica (calcined) prepared with Pluronic P123 at different temperatures: (a) 25, (b) 35, (c) 45, and (d) 55 °C.

(narrow distribution). As the temperature increases, the average size of pure micelles remains rather constant between 25 and 65 °C. It appears that the reduced size observed for hybrid micelles, at lower temperature, is still a proof of the structuring influence of the silicate shell, compared with pure micelles: the hybrid micelles are better defined with silicates than without, and this effect is still more important with a larger amount of silicate (P123/DLS/20).

Beyond this structuring effect, the temperature-dependent evolution is here again influenced by the presence of silicates. Without silicate, the size of the pure micelle remains quite constant, around 20 nm between 25 and 65 °C. In presence of silicate, the micelle size tends to increase, and this effect is proportional to the silicate amount (Fig. 5b). We report in Fig. 6 the scanning electron microscopy (SEM) observation of mesoporous silica prepared at different temperatures with Pluronic P123 [13]. The 35–45 °C synthesis temperature range is a critical domain where the shape of particle and their porous framework changes drastically: below it, mesoporous wormhole silica is obtained with a pore size ranging from 2 to 3 nm. At 40 °C, a major shape restructuring is obtained, with rodlike particles being obtained, and internal hexagonal mesopores (9 nm) being aligned as a honeycomb along the particle main axis. Finally, above 50 °C, an amorphous silica framework is obtained, but with a larger and broader pore size distribution. The current DLS analyses confirm that the silicate hybrid micelles prepared with the Pluronic P123 triblock copolymer stand a major structural change at 40 °C (Fig. 5b). DLS gives only an equivalent hydrodynamic

diameter, but we propose that a major contribution to this apparent size increase is relevant to a sphere-to-rodlike micelle transition, allowed by the presence of silicate, which would explain the isotropic-to-hexagonal transition observed with mesoporous silica at this temperature.

4. Conclusions

Compared with any other synthesis of mesoporous silica, our two-step synthesis involves the intermediate formation of stable silicate hybrid micelles, where silicate oligomers form a diffuse outer shell interacting with the PEO chains of nonionic surfactants [12]. Unlike other inorganic–organic hybrid micelles reported in the literature, these objects display a similar structure and dynamics than pure micelles. Steady-state fluorescence studies show that the internal structure of the micelle remains unchanged (viscosity, internal polarity). Lifetime fluorescence measurements show that the aggregation number is slightly increased with the silicate shell and that the exchange between micelles is also reduced, compared with pure micelles. DLS analyses reveal first that the hybrid micelles display the same dynamics when exposed to temperature variation, than pure micelles. In addition, the presence of a silicate shell tends to reinforce the micelle structure, either at high temperature, close to the CP transition, or at lower temperature (for copolymers with a CMT). Finally, the DLS study of hybrid micelles prepared with Pluronic P123 allowed us to explain the dramatic structural transition observed in the preparation of mesoporous silica, and we ascribed it to a sphere-to-rod

geometry change of the hybrid micelles, before silica condensation.

Acknowledgments

E.P. thanks the Canada Natural Sciences and Engineering Research Council of Canada Agency for financial support (Discovery Grant no. 342 859-2011). The authors are thankful to L. Li and Prof. J. Duhamel for their help in fluorescence spectroscopy.

Appendix A. Supplementary data

Supplementary data related to this article can be found at <http://dx.doi.org/10.1016/j.crci.2016.11.001>.

References

- [1] S. Mann, *J. Mater. Chem.* 5 (7) (1995) 935–946.
- [2] C. Sanchez, H. Arribart, M.-M. Giraud Guille, *Nat. Mater.* 4 (2005) 277–288.
- [3] R. Backov, *Soft Matter* 2 (2006) 452–464.
- [4] Y. Li, J. Ma, H. Zhu, X. Gao, H. Dong, D. Shi, *ACS Appl. Mater. Interfaces* 5 (15) (2013) 7227–7235.
- [5] X. Hu, X. Guan, J. Li, Q. Pei, M. Liu, Z. Xie, X. Jing, *Chem. Commun.* 50 (65) (2014) 9188–9191.
- [6] P. Arosio, J. Thevenot, T. Orlando, F. Orsini, M. Corti, M. Mariani, L. Bordonali, C. Innocenti, C. Sangregorio, H. Oliveira, S. Lecommandoux, A. Lascialfari, O. Sandre, *J. Mat. Chem. B* 1 (39) (2013) 5317–5328.
- [7] G.R. Layrac, M. Destarac, C. Gerardin, D. Tichit, *Langmuir* 30 (32) (2014) 9663–9671.
- [8] K. Yan, H. Li, X. Wang, C. Yi, Q. Zhang, Z. Xu, H. Xu, A.K. Whittaker, *J. Mat. Chem. B* 2 (5) (2014) 546–555.
- [9] L. Zhang, H. Li, L. Wu, *Soft Matter* 10 (35) (2014) 6791–6797.
- [10] L.L. Wang, H.Y. Huang, T.B. He, *J. Controlled Rel.* 213 (2015) E73–E73.
- [11] C. Boissière, A. Larbot, A. van der Lee, P.J. Kooyman, E. Prouzet, *Chem. Mater.* 12 (2000) 2902–2913.
- [12] C. Boissière, A. Larbot, C. Bourgaux, E. Prouzet, C.A. Bunton, *Chem. Mater.* 13 (10) (2001) 3580–3586.
- [13] M.A.U. Martines, E. Yeong, A. Larbot, E. Prouzet, *Micropor. Mesopor. Mat.* 74 (2004) 213–220.
- [14] J. Aubard, P. Levoir, A. Denis, P. Claverie, *Comput. Chem.* 11 (3) (1987) 163–178.
- [15] K. Kalyanasundaram, J.K. Thomas, *J. Am. Chem. Soc.* 99 (7) (1977) 2039–2044.